4P008

多サイクル、および、単一サイクルレーザーパルスによるレーザーアシステッド電子散乱過程における衝突時刻のアト秒精度での決定

[1]東大院理
○歸家令果[1]，石田角太[1]，森本裕也[1]，山内　薫[1]

Determination of collision times with attosecond precision in laser-assisted electron scattering by multi-cycle and single-cycle laser pulses

○Reika Kanya[1], Kakuta Ishida[1], Yuya Morimoto[1], Kaoru Yamanouchi[1]
[1] *Department of Chemistry, School of Science, the University of Tokyo, Japan*

【Abstract】 We introduce two schemes for estimating collision times with attosecond temporal resolutions for laser-assisted electron scattering processes induced by multi-cycle near-infrared laser pulses and single-cycle mid-infrared laser pulses.

【Introduction】 One of the most challenging themes in molecular science is to probe ultrafast changes in geometrical structures of isolated molecules in real time with the atomic-scale spatial resolution. Until now several pioneering attempts have been made for achieving the goal by using newly developed experimental methods such as electron diffraction with ultrashort relativistic electron pulses, X-ray diffraction with X-ray free electron lasers, laser-induced electron diffraction, and laser-assisted electron diffraction as reviewed in Ref. [1]. Recently, we proposed another electron diffraction method called THz-wave assisted electron diffraction (TAED) [2], by which geometrical structures of molecules can be determined with the femtosecond temporal resolution. In the present study, we introduce two methods for achieving the attosecond temporal resolution in estimating collision times in laser-assisted electron scattering (LAES) processes induced by multi-cycle near-infrared laser pulses [3] and single-cycle mid-infrared laser pulses.

【Method】 When LAES processes are induced by multi-cycle laser electric fields expressed as $\boldsymbol{F}_0\cos\omega t$, the mechanism of the LAES process can be described in terms of a dimensionless parameter, ξ, defined by

$$\xi = \frac{e}{m_e\omega^2}\boldsymbol{F}_0\cdot\left(\boldsymbol{k}_i-\boldsymbol{k}_f\right), \tag{1}$$

where $\boldsymbol{k}_i$ and $\boldsymbol{k}_f$ are the wave vectors of the incident electron and the scattered electron, respectively, e is unit charge, m_e is mass of electron. When $|\xi| >> |\Delta E|$, where ΔE is the energy shift of scattered electrons, LAES processes can be described in terms of scattering trajectories of classical mechanical electrons in an laser field. Consequently, the collision time, t_c, *i.e.*, the time when the electron-atom collision occurs, can be expressed as

$$t_c = \pm\omega^{-1}\arccos\left(\frac{\Delta E}{\xi\hbar\omega}\right)+mT, \tag{2}$$

where m is an arbitrary integer and T is the laser field period. Equation (2) shows that the collision time within the optical cycle can be estimated from the energy shift and the deflection angle of scattered electrons.

For LAES processes induced by a single-cycle laser electric field, the differential cross section can be evaluated by the semiclassical formula reported in Ref. [2]. By using the

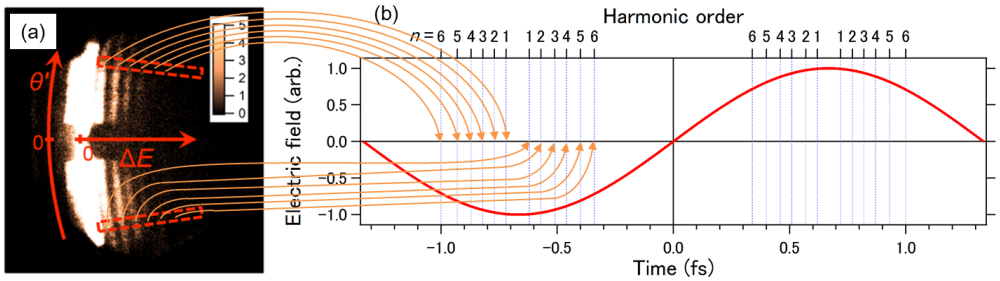

Fig. 1. (a) Energy-resolved angular distributions of scattered electrons. (b) Assignments of collision times for LAES processes yielding the scattering angles of ±11.8°. Red solid line: electric field of the laser field. Blue dotted vertical lines: collision times for the respective harmonic orders, $n = \Delta E / (\hbar\omega)$.

formula, the intensity of electron scattering by H_2^+ in a single-cycle mid-infrared laser pulse (λ = 4 μm, Δt = 13 fs, $I = 1.0\times10^{11}$ W/cm^2) was calculated numerically. In this semiclassical treatment, LAES processes satisfy the relation [2] given by

$$\Delta E = \frac{\hbar e}{m_e}\boldsymbol{A}(t_c)\cdot(\boldsymbol{k}_i - \boldsymbol{k}_f), \tag{3}$$

where $\boldsymbol{A}(t)$ is the vector potential of the laser field. Therefore, if $\boldsymbol{A}(t)$ is known in advance, energy-resolved angular distributions of LAES signals can be converted into time-resolved angular distributions.

【Results and discussion】 Figure 1(a) shows the energy-resolved angular distribution obtained from the measurements of LAES by Xe atoms in a multi-cycle near-infrared laser field (Δt = 100 fs, λ = 800 nm, $I = 8.8\times10^{12}$ W/cm^2) using a 1 keV electron beam [3]. If it is assumed that the scattering occurs around the peak field intensity, the collision times can be estimated by Eq. (2). For example, the collision times for the LAES signals at the scattering angles of ±11.8°, which are expressed as the square areas enclosed by the broken lines in Fig. 1(a), are shown by the arrows in Fig. 1(b) for the respective harmonic orders, $n = \Delta E / (\hbar\omega)$, showing that slight differences in the collision times of the order of 10 attoseconds can be discriminated.

Figure 2(a) shows the signal distributions of electrons scattered by dissociating H_2^+ molecular ions. By converting the energy shift axis in Fig. 2(a) to the collision time axis, the time-dependent electron diffraction patterns are obtained. From the analysis of the electron diffraction patterns, the time-dependent internuclear distance, $R(t)$, of H_2^+ is retrieved. As shown in Fig. 2(b), the retrieved $R(t)$ (the red solid line) is in good agreement with the initially given $R(t)$ (the black solid line), showing that ultrafast structural changes in geometrical structure of molecules can be probed with the attosecond temporal resolution.

【Acknowledgements】 This work was supported by JSPS KAKENHI Grant Numbers JP26288004, JP15H05696, and JP17H03004, and by a grant from Morino Foundation for Molecular Science.

【References】

[1] J. Xu, C. I. Blaga, P. Agostini, and L. F. DiMauro, *J. Phys. B* **49**, 112001 (2016).

[2] R. Kanya and K. Yamanouchi, *Phys. Rev. A* **95**, 033416 (2017).

[3] K. Ishida, Y. Morimoto, R. Kanya, and K. Yamanouchi, *Phys. Rev. A* **95**, 023414 (2017).

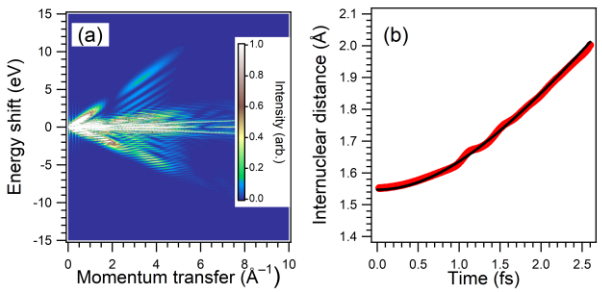

Fig. 2. (a) Signal distributions of electrons scattered by dissociating H_2^+ molecular ions.
(b) Time-dependent internuclear distance, $R(t)$. Black solid line: initially given $R(t)$, Red solid line: $R(t)$ retrieved from the analysis of the intensity distributions in Fig. 2(a).